Effect of substrate temperature on the morphological, structural, and optical properties of RF sputtered $Ge_{1-x}Sn_x$ films on Si substrate*

H Mahmodi[1,†] and M R Hashim[2]

[1] Nano-Optoelectronics Research Laboratory, School of Physics, Universiti Sains Malaysia, 11800 USM, Pulau Penang, Malaysia
[2] Institute of Nano Optoelectronics Research and Technology (INOR), Universiti Sains Malaysia, 11800 USM, Pulau Penang, Malaysia

(Received 14 October 2016; revised manuscript received 26 January 2017; published online 6 April 2017)

In this study, $Ge_{1-x}Sn_x$ alloy films are co-sputtered on Si(100) substrates using RF magnetron sputtering at different substrate temperatures. Scanning electron micrographs, atomic force microscopy (AFM), Raman spectroscopy, and x-ray photoemission spectroscopy (XPS) are conducted to investigate the effect of substrate temperature on the structural and optical properties of grown GeSn alloy films. AFM results show that RMS surface roughness of the films increases from 1.02 to 2.30 nm when raising the substrate temperature. This increase could be due to Sn surface segregation that occurs when raising the substrate temperature. Raman spectra exhibits the lowest FWHM value and highest phonon intensity for a film sputtered at 140 °C. The spectra show that decreasing the deposition temperature to 140 °C improves the crystalline quality of the alloy films and increases nanocrystalline phase formation. The results of Raman spectra and XPS confirm Ge–Sn bond formation. The optoelectronic characteristics of fabricated metal-semiconductor-metal photodetectors on sputtered samples at room temperature (RT) and 140 °C are studied in the dark and under illumination. The sample sputtered at 140 °C performs better than the RT sputtered sample.

Keywords: GeSn, magnetron sputtering, Raman scattering, x-ray photoemission spectroscopy

PACS: 68.55.ag, 68.55.–a, 74.25.nd, 82.80.Pv **DOI:** 10.1088/1674-1056/26/5/056801

1. Introduction

A $Ge_{1-x}Sn_x$ alloy film is an important material in the development of group-IV semiconductor heterostructures for both optoelectronic and high-performance electronic devices. The $Ge_{1-x}Sn_x$ alloy system has the potential to be the most important materials used in the next generation of infrared detectors.[1] This requires additional improvements in GeSn alloy synthesis and growth parameters optimization. The most recent progress in GeSn alloy applications include the fabrication of a GeSn laser,[2] GeSn light emitting diodes,[3] p-GeSn/n-Ge diodes,[4] GeSn photoconductors,[5] and GeSn p–i–n photodetectors.[6] This alloy is a good candidate for semiconductor materials that can be grown on a Si substrate.

Despite difficulties in growing epitaxial $Ge_{1-x}Sn_x$-like low solubility of Sn and Ge ($> 1\%$),[7] Sn surface segregation,[8] and huge lattice mismatch between α-Sn- and Ge-specific[9] non-equilibrium growth technique were developed to grow this alloy. These methods include molecular beam epitaxy,[10] chemical vapour deposition,[11,12] and magnetron sputtering.[6,13] The sputtering method is used extensively in the deposition of crystalline and amorphous semiconductors, particularly for GeSn alloys.[6,14,15] This techniques allows us to sputter semiconductor alloys[16,17] and to control easily the deposition parameters such as gas flow, substrate temperature, sputtering power, alloy composition, and deposition time.[13,18] The substrate temperature is a crucial factor that controls Sn surface segregation and affects the $Ge_{1-x}Sn_x$ film crystalline quality during growth.

Our research aims to investigate the role of the substrate temperature on the crystalline state of sputtered $Ge_{1-x}Sn_x$ films. The alloy films are co-sputtered simultaneously from high purity Ge and Sn targets onto a Si substrate by using RF magnetron sputtering at various substrate temperatures (T_s). The results show improved optical and structural characteristics of GeSn films sputtered at a low elevated deposition temperature. In addition, the optoelectronic characteristics of fabricated metal-semiconductor-metal photodetectors (MSM PDs) on GeSn are studied in the dark and under illumination to investigate the substrate temperature effect and potential applications of GeSn in optoelectronic devices. The MSM photodetector is a device that has been widely investigated because of its fast response, low dark currents, small capacitance, and large active area for photodetection.[19]

2. Experimental details

Si substrates were cleaned using the cleaning method before film deposition, which has been developed by Radio Corporation of America (RCA).[20] $Ge_{1-x}Sn_x$ alloys were deposited in an RF magnetron sputtering system (Edwards A500, UK) on n-Si (100) substrates with a base pressure of 2.0×10^{-5} mbar and Ar of high purity (99.999%), at room temperature, 140, 160, 180, and 200 °C. Both Ge (99.999%) and Sn (99.999%) targets had a diameter of 10 cm and were set 10 cm from the substrate. The magnetrons were located in planar configuration. The targets were co-sputtered under an

*Project supported by the Universiti Sains Malaysia (Grant No. 1001/PFIZIK/846072).
†Corresponding author. E-mail: hadi.mahmodi@gmail.com
© 2017 Chinese Physical Society and IOP Publishing Ltd

RF sputtering power of 100 W and 15 W for Ge and Sn, respectively. The monitored voltage for Ge and Sn RF sources were 85 and 50 V, respectively.

To fabricate the MSM PD, metal deposition was conducted to build metal contacts on the GeSn films. The PD device has two interdigitated Schottky contacts (electrode), in which each electrode has four fingers. The width and length of each finger are 230 μm and 3.3 mm, respectively. The spacing between each finger is 400 μm. Using vacuum thermal evaporation, nickel Schottky contacts were deposited by using a metal mask (finger pattern). This was followed by annealing the samples in flowing nitrogen at 400 °C for 5 min. The Ni Schottky contact thickness was approximately 200 nm.

Field emission scanning electron microscopy (FESEM) (model FEI-Nova NanoSEM 450) and atomic force microscopy (AFM) were used to analyse the surface morphology of thin films. Energy-dispersive x-ray spectroscopy (EDX) was used to identify the elements present in the samples at 10 kV. X-ray photoemission spectroscopy (XPS) (Axis Ultra DLD XPS, Kratos) was used to identify the elements present in the samples. Raman spectroscopy was performed using a Jobin–Yvon (HR800UV) spectrometer, in which the samples were excited at room temperature with an argon ion laser (514.5 nm, 20 mW). A high-resolution x-ray diffractometer (HR-XRD) system (X'Pert3040) was used exclusively for crystallographic investigation of the samples. Electrical measurements were performed at RT using a computer-controlled integrated SourceMeter (Keithley 2400).

3. Results and discussion

3.1. Film compositional analysis

Based on EDX spectral results, the Sn composition (atomic) of the sputtered layers was obtained. The spectra image obtained by means of typical EDX of the as-sputtered sample (Fig. 1) shows that four basic peaks were formed at 0.52, 1.18, 1.73, and 3.44 keV. These match the spectral lines of O, Ge, Si, and Sn, respectively. Si originated from the substrate and O was most likely caused by the surface oxidation of the GeSn film when exposed to air after deposition. The Sn concentration of sputtered films are shown in Table 1. Note that by increasing the substrate temperature, the Sn composition for the RT sputtered sample increased slightly from 5.7% to more than 13% at 180 °C, which could be the result of the Sn segregation of the top layers of the films during film growth. However, the Sn composition of the sample sputtered at 200 °C was lower than that of the samples sputtered at a lower elevated temperature (140 °C$\leq T_s \leq$ 180 °C). This may be because of the high temperature applied to the substrate, which induced considerable Sn migration and desorption from the film surface.[21] It was reported that Sn migration and desorption depend strongly on deposition temperature, which influence the depth distribution of Sn in the GeSn layer.

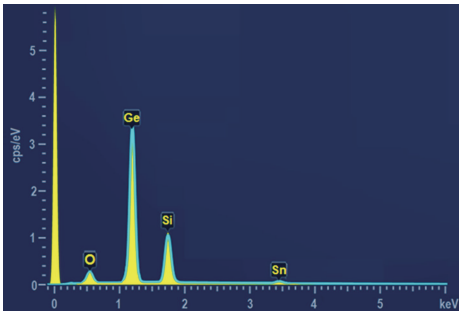


Fig. 1. (color online) Typical EDX spectra of the RT sputtered $Ge_{1-x}Sn_x$ sample.

Table 1. Ge and Sn atomic concentration of $Ge_{1-x}Sn_x$ sample sputtered at various substrate temperatures.

Sample	Atomic concentration/%	
	Ge	Sn
RT	94.30	5.70
140 °C	89.80	10.2
160 °C	88.20	11.8
180 °C	86.60	13.4
200 °C	99.30	0.70

3.2. Surface morphology

Figure 2 shows FESEM and three-dimensional AFM images of the $Ge_{1-x}Sn_x$ films sputtered at room and elevated temperatures. All films showed agglomerates of clusters and a densely packed morphology. However, these clusters were formed as a result of a coalescence of small grains. The RT sputtered sample had a thickness of 270 nm. The thickness of the GeSn thin films was 221, 233, 247, and 201 nm for the sputtered samples at 140, 160, 180, and 200 °C, respectively. To further analyse the surface morphology, we employed AFM. In all samples, the surface formed a hillock structure. The AFM results reveal the effect of substrate temperature variations. As shown in Table 2, the lowest surface roughness of 1.02 nm was obtained for the RT sputtered sample, whereas for the other samples, it increased from 1.26 to 2.30 nm when raising the substrate temperature. This suggests that the increment of RMS surface roughness for the samples that sputtered at an elevated substrate temperature was due to the Sn surface segregation. Sn tends to segregate to the film surface during deposition because of the surface free energy difference and limited solubility between Sn and Ge.[22,23] We observed that, among the deposited films with substrate heating, the sputtered sample at 140 °C had the lowest RMS surface value. Therefore, we could conclude that this sample had less Sn surface segregation.

Table 2. RMS surface roughness of the GeSn films sputtered at different substrate temperatures.

Samples	RT	140 °C	160 °C	180 °C	200 °C
Surface roughness/nm	1.02	1.26	1.65	1.83	2.30

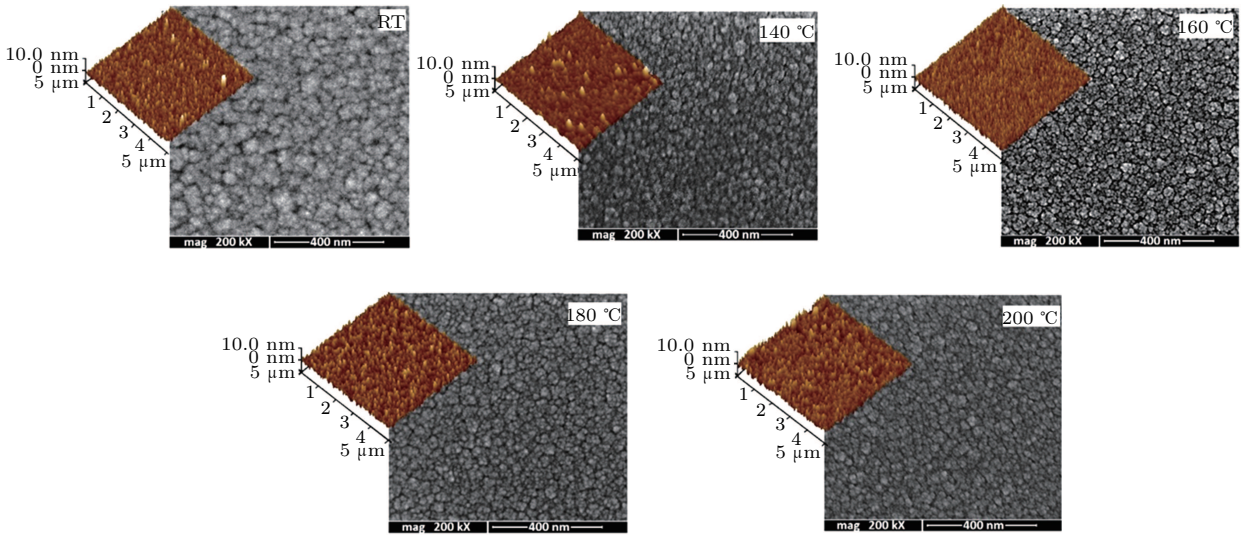


Fig. 2. (color online) FESEM and AFM images of the GeSn alloy films sputtered at various substrate temperatures.

3.3. Raman spectroscopy

Figure 3 shows the Raman spectra of $Ge_{1-x}Sn_x$ samples deposited at different substrate temperatures. Raman frequency modes corresponding to Ge–Ge, Ge–Sn, and Sn–Sn modes were expected to be observed in GeSn alloy films. Ge–Sn LO peaks, which are usually around 260 cm^{-1}, were not found in our spectra. Since the laser wavelength of 532 nm, as used in this study, is far from the resonance condition with the $E_1 - E_1 + \Delta_1$ optical transitions, as suggested by D'Costa *et al.*,[24,25] a Ge–Sn bond was observed when the GeSn layer was excited by a laser with wavelengths of 633 nm[26,27] and 647.1 nm.[25] These wavelengths enable a clear detection of all first-order vibrational modes. Thus, the main observed peak could be correctly indexed to Ge–Ge vibrations. A previous study reported that an Sn–Sn-like mode is observed between 100–200 cm^{-1}.[25] No clear visible sign of the Sn–Sn peak appears. However, a small bump can be seen in the sputtered sample at RT, 140, and 160 °C at approximately 150 cm^{-1}.

The peak position of the Ge–Ge mode shifted during substrate temperature variations, as shown in Table 3. For all samples, the Ge–Ge peak shifted to a higher wave number compared to that of the RT sputtered sample. The Ge–Ge peak of the RT sputtered sample was located at 264.24 cm^{-1}, which suggested it was in an amorphous phase.[28,29] The Ge–Ge peak shifted to a higher wave number that approximated the bulk c-Ge (301.01 cm^{-1}) when the deposition temperature increased. However, the Raman peak of the sample that was sputtered at 160 °C was closer to the bulk Ge crystal as compared to other samples. In semiconductor alloys, the Raman frequency shift is known to be affected mostly by the compositional variation and strain.[30,31]

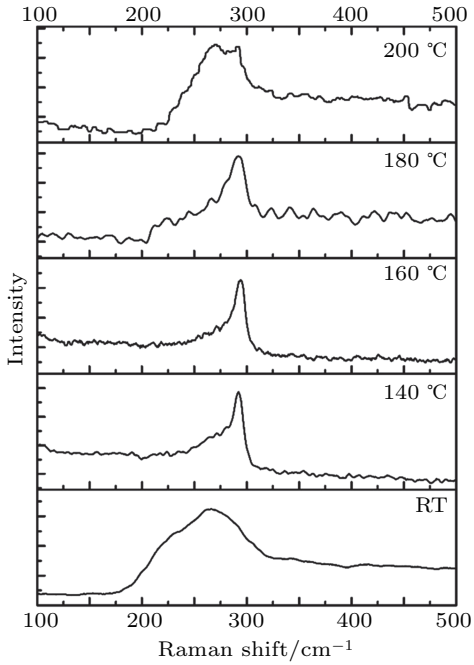


Fig. 3. Raman spectra of the GeSn thin films sputtered at RT and elevated substrate temperatures.

Table 3. Ge–Ge phonon modes detected in Raman spectra of GeSn films sputtered at various substrate temperatures. The frequency shift value is compared to the RT sputtered sample.

Sample	Peak wave number/cm^{-1}	Peak intensity/a.u.	FWHM /cm^{-1}	Shift /cm^{-1}
RT	264.24	485	82.62	–
140 °C	292.17	970	16.12	27.93
160 °C	294.10	794	16.83	29.86
180 °C	291.08	96	24.76	28.72
200 °C	290.79	75	44.13	26.55

Asymmetric broadening as a result of the variation in substrate temperatures during deposition could be observed. The RT sputtered sample had the broadest curve, with an FWHM value of 82.62 cm^{-1}. The broad and more left-shifted curve of

this sample indicates the amorphous nature of the film, which is comparable to other reported studies.[28] The broadening of the Raman spectra resulted from the disordered crystals (or amorphous phases), which originated from the superposition of spectra with shifted frequencies.[32] In addition, the asymmetric broadening of the Ge–Ge peak was because the substrate temperature increased from 140 to 200 °C. As shown in Table 3, the FWHM of the sample that sputtered at 140 °C was 16.12 cm^{-1}, which is smaller than that sputtered at 200 °C, the FWHM value for which was 44.13 cm^{-1}. It is suggested this is because of the Sn surface segregation during deposition, which degrades the film crystalline quality of the high-temperature sputtered sample. Although the FWHM value of both samples that were sputtered at 140 and 160 °C are nearly the same, the phonon intensity of the sputtered sample at 140 °C is higher. Therefore, an enhanced crystallite quality of GeSn was observed in the sample sputtered at the lowest elevated temperature of 140 °C.

Substrate temperature variation has an effect on the phonon intensity of the Ge–Ge peak. As shown in Table 3, the phonon intensity of the sample sputtered at 140 °C was higher than that sputtered at 200 °C. This sample even exhibited lower phonon intensity than did the RT sputtered sample. This shows that higher interactions with incident photons occur in the sputtered film at 140 °C, which means the crystallite structure of GeSn film is enhanced.

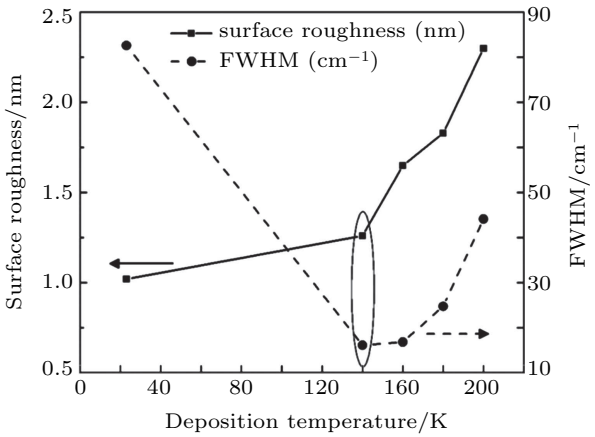


Fig. 4. FWHM and surface roughness of the sputtered GeSn films at different deposition temperatures.

In addition, figure 4 shows that increasing the substrate temperature resulted in an increase in the surface roughness and Ge–Ge curve FWHM. The sample with the lowest FWHM exhibited a low RMS surface roughness among the samples grown at elevated temperatures. Because the surface roughness increased as a result of Sn surface segregation, we can conclude that this sample encountered less Sn surface segregation compared to the other samples. Thus controlling the deposition temperature resulted in low Sn surface segregation and improved the crystalline quality of the alloy film.

3.4. High-resolution x-ray diffraction

Figure 5 shows the XRD diffraction pattern of the sputtered GeSn alloy on a Si substrate at different substrate temperatures. The sharpest peak observed at $2\theta = 69.32°$ is attributed to the Si (400) substrate. For the GeSn layer sputtered at $T_s = 140$ °C, a diffraction pattern at $2\theta = 26.37°$ was observed, which was between the 2θ angles for a-Sn (111) and c-Ge (111), 23.7°–27.3°. This peak is attributed to the cubic $Ge_{1-x}Sn_x$ (111) structure,[33] which shows evidence of crystallization. No clear diffraction pattern for GeSn was observed in the other samples, indicating that they were in an amorphous phase. However, another observed feature is a weak and low intensity peak at $2\theta = 32.5°$ for $T_s = 200$ °C, which is owned to the Sn(101). The observation of this peak could be attributed to considerable Sn surface segregation.

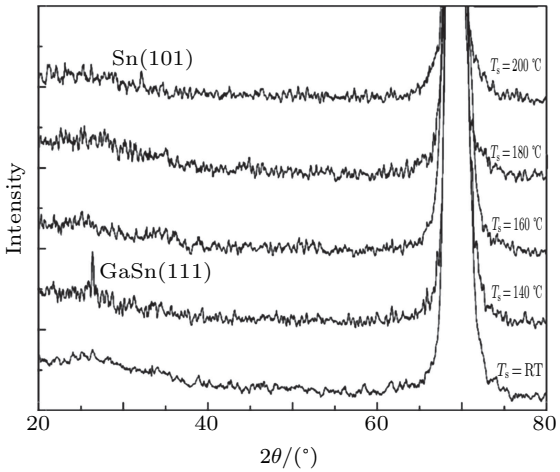


Fig. 5. X-ray diffraction (XRD) spectra of GeSn alloy sputtered at different substrate temperatures: RT, 140, 160, 180, and 200 °C.

3.5. X-ray photoemission spectroscopy

XPS analysis of the sputtered sample film at a substrate temperature of 140° is shown in Fig. 6. The observed peaks in this spectrum can be assigned to Ge, Sn, and O. Figure 6(a) reveals that Ge has two distinct peaks at 29.80 and 33.12 eV, which belong to Ge and GeO_2 or a mixture of GeO and GeO_2, respectively. Figure 6(b) reveals two peaks for Sn at 487.43 and 495.95 eV. The Sn $3d_{5/2}$ peak belongs to Sn itself (Sn $3d_{5/2}$) and the other peak could be assigned to Sn $3d_{3/2}$, which derives from GeSn or SnO_2. The observation of GeO_2 and SnO_2 on the film surface is because of exposure of samples to the atmosphere[34] or the reaction between residual oxygen molecules and Ge or Sn atoms inside the vacuum chamber during growth.[35] This observation is in good agreement with the XPS database.[36]

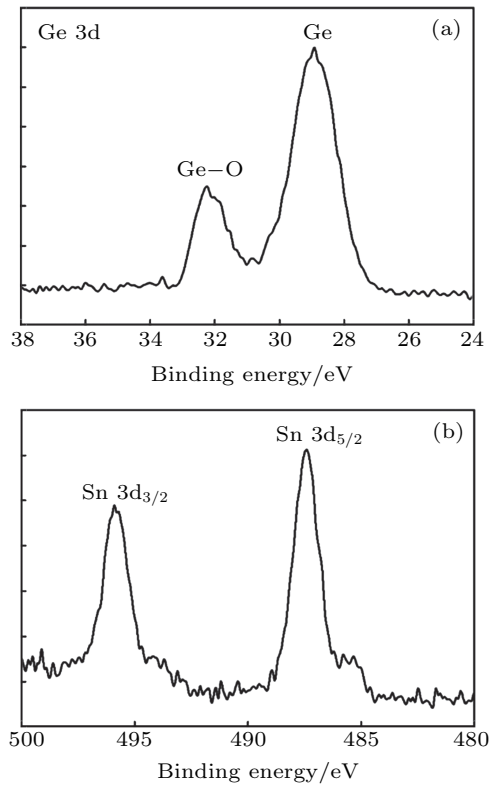


Fig. 6. XPS spectra of the sputtered GeSn film at 140 °C: (a) Ge 3d spectra, and (b) Sn 3d spectra.

3.6. Current–voltage characteristics

The current–voltage (I–V) characteristics of MSM photodetectors on the sputtered samples at RT and 140 °C were studied and are shown in Fig. 7. The electrical properties of the sputtered films were investigated based on the I–V characteristics measured in the dark (I_{Dark}) and under illumination of visible light (I_{Photo}). The current gain (i.e., the ratio of photocurrent to dark current) is displayed in Fig. 7(b). The current gain is calculated from current–voltage characteristics using the equation Gain $= I_{\text{Photo}}/I_{\text{Dark}}$.

As shown in Fig. 7(a), the response of the MSM PDs increased with the bias voltage and saturated gradually at a voltage above 1.0 V. This was because of the swiping out of all carriers toward the device contacts. In both PDs, the fact that the photocurrent produced a higher current than that generated in the dark is clear. More importantly, the sample sputtered at 140 °C produced a lower dark current than did the RT sputtered sample by a factor of nearly less than two (from 0.95 to 0.53 μA) and a higher photocurrent by a factor of approximately 2 (from 13 to 24 μA) at a 5 V bias. By comparing the current at a 5 V bias for the 140 °C sputtered sample, we found the photocurrent to be 2.38×10^{-5} A. By contrast, for the dark sample, 5.11×10^{-7} A was observed. This finding indicates that under illumination, more electron–hole pairs are created in the GeSn film, which greatly increases the current density.

Figure 7(b) shows the current gain for both MSM PDs. As shown, at a 1.0 V bias, the current gain of the sample sputtered at 140 °C improved by more than 80 times compared to the RT sputtered sample. Although it gradually decreased as bias voltage increased because of series resistance, it remained at a good level. The greater enhancement of the current gain may be related to the enhanced crystalline quality of the 140 °C sputtered film as compared to the RT sputtered sample, which agrees with the Raman spectrum analysis. In addition, this indicates high photo-responsivity of the GeSn film sputtered at a low elevated temperature. Thus, we showed the effect of substrate temperature on the crystalline phase formation in the MSM PD and observed that the sample sputtered at an elevated temperature exhibited better performance.

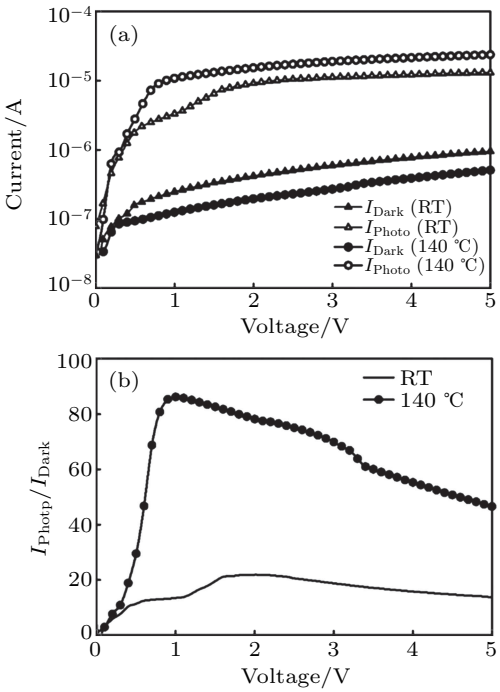


Fig. 7. (a) Current–voltage characteristics of the fabricated MSM photodetectors on the samples sputtered at RT and 140 °C, which were measured in the dark (I_{Dark}) and under illumination (I_{Photo}) with (b) the current gain ($I_{\text{Photo}}/I_{\text{Dark}}$).

4. Conclusion

The GeSn alloy films were co-sputtered on Si substrates by RF magnetron sputtering and the effects of substrate temperature on the morphological, structural, and optical properties of GeSn layers were investigated. The AFM results showed that the films sputtered at a lower elevated temperature of 140 °C exhibited less RMS surface roughness. In addition, Raman spectroscopy results revealed that this sample had the smallest FWHM value and the highest phonon intensity, thus indicating improved crystalline quality of the alloy film. The XRD result indicates that at $T_s = 140$ °C, the nanocrystalline GeSn was grown with (111) preferred orientation. XPS and Raman spectra results confirmed the formation of GeSn bonds, which demonstrates that Sn was incorporated in the Ge matrix. The electrical characteristics of the MSM PD fabricated on the sample sputtered at 140 °C displayed a lower dark current and higher current gain compared to the RT sputtered sample. The results reveal the role of substrate temperature in controlling

Sn surface segregation and thereby improving the GeSn crystalline quality.

References

[1] Oehme M, Widmann D, Kostecki K, Zaumseil P, Schwartz B, Gollhofer M, Koerner R, Bechler S, Kittler M, Kasper E and Schulze J 2014 *Opt. Lett.* **39** 4711

[2] Wirths S, Geiger R, von den Driesch N, Mussler G, Stoica T, Mantl S, Ikonic Z, Luysberg M, Chiussi S, Hartmann J M, Sigg H, Faist J, Buca D and Grützmacher D 2015 *Nat. Photon.* **9** 88

[3] Du W, Hou Z, Ghetmiri S A, Mosleh A, Conley B R, Nazzal A, Soref R A, Sun G, Tolle J, Margetis J, Naseem H A and Yu S Q 2014 *Appl. Phys. Lett.* **104** 241110

[4] Baert B, Gupta S, Gencarelli F, Loo R, Simoen E and Nguyen N D 2015 *Solid-State Electron.* **110** 65

[5] Conley B R, Mosleh A, Ghetmiri S A, Du W, Soref R A, Sun G, Margetis J, Tolle J, Naseem H A and Yu S Q 2014 *Opt. Express* **22** 15639

[6] Zheng J, Wang S, Liu Z, Cong H, Xue C, Li C, Zuo Y, Cheng B and Wang Q 2016 *Appl. Phys. Lett.* **108** 033503

[7] Thurmond C D, Trumbore F A and Kowalchik M 1956 *J. Chem. Phys.* **25** 799

[8] Pukite P R, Harwit A and Iyer S S 1989 *Appl. Phys. Lett.* **54** 2142

[9] Wang W, Su S, Zheng J, Zhang G, Xue C, Zuo Y, Cheng B and Wang Q 2011 *Appl. Surf. Sci.* **257** 4468

[10] Nikolenko A S, Strelchuk V V, Safriuk N V, Kryvyi S B, Kladko V P, Oberemok O S, Borkovska L V and Sadofyev Y G 2015 *Thin Solid Films* **613** 68

[11] Gencarelli F, Shimura Y, Kumar A, Vincent B, Moussa A, Vanhaeren D, Richard O, Bender H, Vandervorst W, Caymax M, Loo R and Heyns M 2015 *Thin Solid Films* **590** 163

[12] Soref R, Kouvetakis J, Tolle J, Menendez J and D'Costa V 2007 *J. Mater. Res.* **22** 3281

[13] G. Ming-Wei, Y. Chao, W. Xiang-Ying, H. Yi-Song, G. Jia-Min, Y. Pei-Fang, 2016 *Chin. Phys. B* 25 075202

[14] de Guevara H P L, Rodriguez A G, Navarro-Contreras H and Vidal M A 2003 *Appl. Phys. Lett.* **83** 4942

[15] Tsukamoto T, Hirose N, Kasamatsu A, Mimura T, Matsui T and Suda Y 2015 *J. Mater. Sci.* **50** 4366

[16] Zhang X J, Yuan H M, Wang Q P, Wang T and Ma H L 2010 *Chin. Phys. B* **19** 018102

[17] Li G F, Hu J, Lv H, Cui Z J, Hou X W, Liu S B and Du Y Q 2016 *Chin. Phys. B* **25** 027304

[18] Samavati A, Ghoshal S K and Othaman Z 2012 *Chin. Phys. Lett.* **29** 048101

[19] Zhou J J, Jiang R L, Sha J, Liu J, Shen B, Zhang R and Zheng Y D 2003 *Chin. Phys.* **12** 785

[20] Reinhardt K A and Kern W 2008 *William* Andrew

[21] Taoka N, Asano T, Yamaha T, Terashima T, Nakatsuka O, Costina I, Zaumseil P, Capellini G, Zaima S and Schroeder T 2015 *Appl. Phys. Lett.* **106** 061107

[22] Harwit A, Pukite P R, Angilello J and Iyer S S 1990 *Thin Solid Films* **184** 395

[23] Wegscheider W, Olajos J, Menczigar U, Dondl W and Abstreiter G 1992 *J. Cryst. Growth* **123** 75

[24] D'Costa V R, Tolle J, Poweleit C D, Kouvetakis J and Menéndez J 2007 *Phys. Rev. B* **76** 035211

[25] D'Costa V R, Tolle J, Roucka R, Poweleit C D, Kouvetakis J and Menéndez J 2007 *Solid State Commun.* **144** 240

[26] Oehme M, Buca D, Kostecki K, Wirths S, Holländer B, Kasper E and Schulze J 2013 *J. Cryst. Growth* **384** 71

[27] Fournier-Lupien J H, Mukherjee S, Wirths S, Pippel E, Hayazawa N, Mussler G, Hartmann J M, Desjardins P, Buca D and Moutanabbir O 2013 *Appl. Phys. Lett.* **103** 263103

[28] Li H, Brouillet J, Salas A, Wang X and Liu J 2013 *Opt. Mater. Express* **3** 1385

[29] Lieten R R, Fleischmann C, Peters S, Santos N M, Amorim L M, Shimura Y, Uchida N, Maeda T, Nikitenko S, Conard T, Locquet J P, Temst K and Vantomme A 2014 *ECS J. Solid State Sci. Tech.* **3** 403

[30] Tsang J C, Mooney P M, Dacol F and Chu J O 1994 *J. Appl. Phys.* **75** 8098

[31] Hossain M Z and Johnson H T 2010 *J. Appl. Phys.* **107** 1

[32] Sorianello V, Colace L, Assanto G and Nardone M 2011 *Microelectron. Eng.* **88** 492

[33] Hirofumi F, Hiroaki M, Toshio N, Takeshi I and Yukio O 1986 *Jpn J. Appl. Phys.* **25** 1312

[34] Molle A, Bhuiyan M N K, Tallarida G and Fanciulli M 2006 *Appl. Phys. Lett.* **89** 083504

[35] Zhang D, Liao Y, Li J, Wen T, Jin L, Wang X and Kolodzey J 2016 *J. Alloy. Compound.* **684** 643

[36] Castain J 1992 *Hand Book of x-ray Photoelectron Spectroscopy* (Minnesota, USA: Perkin-Elmer Corp.)